The ground-state configurations of arbitrary spin- ***S*** Ising models with axial next-nearest-neighbour interactions

1996 J. Phys. A: Math. Gen. 29 949

(http://iopscience.iop.org/0305-4470/29/5/011)

J. Phys. A: Math. Gen. **29** (1996) 949–962. Printed in the UK

The ground-state configurations of arbitrary spin-S Ising models with axial next-nearest-neighbour interactions

Y Muraoka†, K Oda‡, J W Tucker§‖ and T Idogaki‡

† Department of General Education, Ariake National College of Technology, Omuta, Fukuoka 836, Japan

‡ Department of Applied Science, Faculty of Engineering 36, Kyushu University, Fukuoka 812-81, Japan

§ Department of Physics, The University of Sheffield, Sheffield S3 7RH, UK

Received 4 September 1995

Abstract. A lemma, proposed by Morita and Horiguchi to determine the ground-state phase diagram of the spin-$\frac{1}{2}$ axial next-nearest-neighbour Ising (ANNNI) model, is generalized to arbitrary spin. A prescription for finding the 'fundamental spin arrangements' which are the basic building blocks for the ground state is given, and the method of constructing the ground state is explained. The method is applied to a determination of the magnetic ground-state phase diagrams of the ANNNI model with arbitrary spin, various one-dimensional spin-1 ANNNI models with higher-order axial spin interactions, and to the same systems with interchain couplings in two and three dimensions.

1. Introduction

The axial next-nearest-neighbour Ising (ANNNI) model with bilinear exchange [1] has attracted many investigators on account of the fact that it is a simple model that exhibits spatially modulated phases. Spin-S Ising models with higher-order next-nearest-neighbour interactions may be regarded as extended ANNNI models, and are also expected to exhibit a variety of interesting phase transitions and ordered states.

Determination of the ground-state spin configuration is a fundamental and, in the case of systems with competing interactions, a non-trivial problem, in the study of phase transitions. For one-dimensional Ising systems with periodic boundary conditions, the eigenvalues of the transfer matrix can be used to determine the ground-state energy [2, 3]. However, for a spin-S system with next-nearest-neighbour interactions, the size of the transfer matrix is $(2S+1)^2 \times (2S+1)^2$. Thus for a system with large spin, or one having even more extended interactions, it becomes very difficult to calculate the eigenvalues analytically due to the size of the matrix involved. As the ground-state configuration is determined indirectly from the exact ground-state energy in this method, the transfer matrix approach is no longer feasible for this purpose. For systems with macroscopic ground-state degeneracy [4], a direct determination of the spin configurations is required.

The one-dimensional $S = \frac{1}{2}$ ANNNI model in an external field may be described by the Hamiltonian

$$H = -\sum_i (J_1 S_i S_{i+1} + J_2 S_i S_{i+2} + h S_i) \qquad \text{[2–2] model} \tag{1}$$

‖ Author to whom correspondence should be addressed.

0305-4470/96/050949+14$19.50

where J_1 and J_2 are the nearest and next-nearest-neighbour exchange interactions, and h is the external field (in units where the splitting factor and Bohr magneton are unity). Throughout this paper, it is tacitily assumed that periodic boundary conditions are imposed on all the systems.

For the above model, Morita and Horiguchi [5] proved the lemma that an arbitrary spin configuration can be regarded as composed of a sequence of only six kinds of spin arrangements, and that the total energy, E, is a linear combination of the energy elements, ϵ_i, belonging to them. Specifically,

$$E = n_+\epsilon_+ + n_-\epsilon_- + 2n_{+-}\epsilon_{+-} + 3n_{+--}\epsilon_{+--} + 3n_{+-+}\epsilon_{+-+} + 4n_{+--+}\epsilon_{+--+} \tag{2}$$

where the subscripts $+-$, etc indicate the spin arrangements. n_i is the number of times the particular arrangement, i, occurs in the arbitrary spin configuration, and the energies ϵ_i are the energies per spin in each arrangement.

In this paper we adopt the concept of *a fundamental spin arrangement* and generalize the above lemma to be applicable to all one-dimensional extended ANNNI models of arbitrary spin S with nearest and various next-nearest-neighbour interactions, described by

$$\mathcal{H} = -\sum_i H(S_i, S_{i+1}, S_{i+2}) \tag{3}$$

where $S_i = S, S-1, \ldots, -S$. $H(S_i, S_{i+1}, S_{i+2})$ may include not only the bilinear exchange interactions S_iS_{i+1}, but also higher-order spin interactions $S_i^2S_{i+1}^2$, $S_iS_{i+1}^2S_{i+2}$, for example. This extended lemma is then used, firstly, to find the ground-state phase diagram of various one-dimensional extended ANNNI models exactly, and secondly, to find the ground state of axial two- and three-dimensional models having ferromagnetic interchain couplings. As a check on our technique, we have compared our results with those of a direct computer search for the ground-state configuration of finite chains.

The arrangement of the paper is as follows. In section 2.1 the extended lemma is proposed, and a demonstration of its use on a specimen configuration is presented. Section 2.2 gives the prescription for finding the fundamental spin arrangements into which an arbitrary configuration may be broken. For the cases of $S = \frac{1}{2}$ and $S = 1$ all the fundamental spin arrangements are found. The construction of the ground state is described in section 2.3, and the results for the ground-state phase diagrams of the one-dimensional and higher-dimensional extended ANNNI models are presented in sections 3.1 and 3.2, respectively. Finally, in section 4, the results are summarized and concluding remarks made.

2. Basic theory

2.1. A lemma

We introduce a *basic dividing rule* for Ising chains of arbitrary spin quantum number, having only nearest- and next-nearest-neighbour spin interactions. (The slight modification required for systems with a more extensive range of interactions is given in section 4.) A one-dimensional spin arrangement on which periodic boundary conditions are imposed will be called a *closed chain*. Denoting the spin states of S_i by A, B, C, etc, the basic dividing rule can be described with the help of figure 1. Proceeding along the chain, one looks at the sequence of states associated with each pair of nearest-neighbouring spins in turn. If a sequence of states repeats, one cuts the closed chain immediately to the left of the first spin in each of the repeating segments. Periodic boundary conditions are then imposed on each of the broken parts to form new closed chains. Thus in figure 1, with the observation

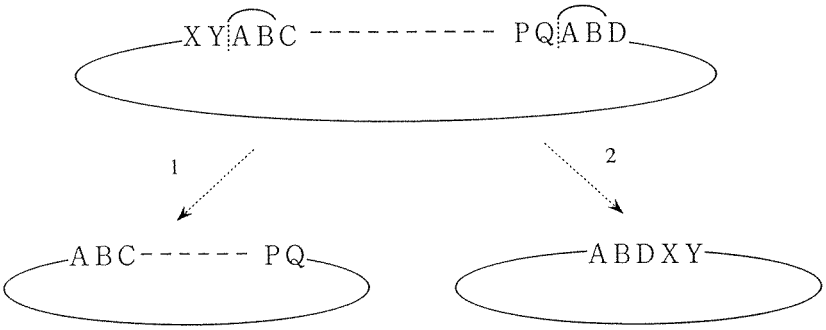

Figure 1. The basic dividing rule for arbitrary spin quantum number. A, B, ..., indicate different spin states.

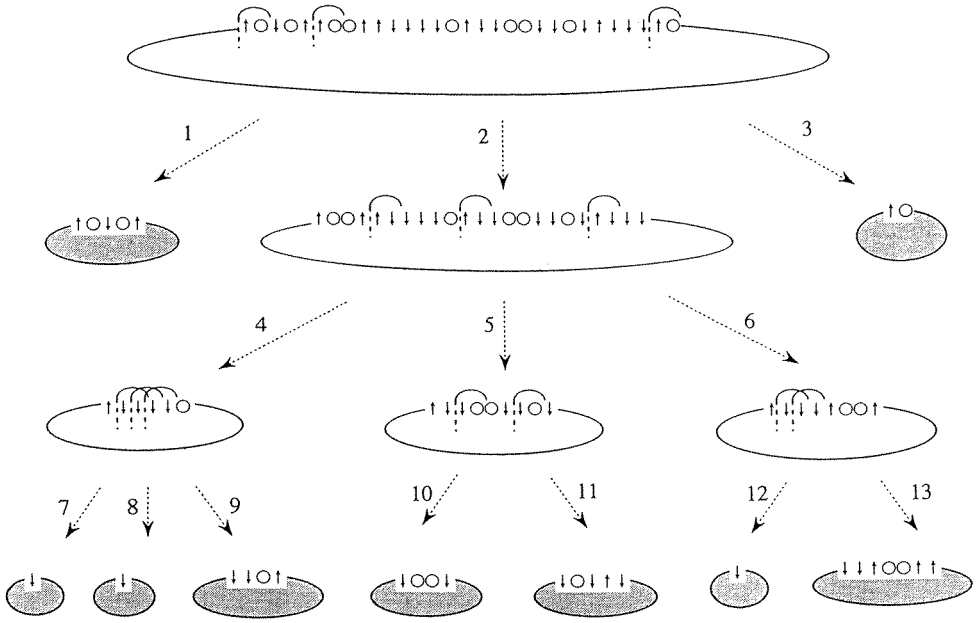

Figure 2. An example of a decomposition of a spin-1 configuration into fundamental spin arrangements, for a system with nearest- and next-nearest-neighbour interactions.

that segment AB occurs twice, the initial closed chain is broken to the left of each AB to give two new chains as shown. It is easily verified, that for systems having only nearest- and next-nearest-neighbour interactions, that the energy of the original closed chain is equal to the sum of the energies of the two shorter closed chains. One then looks for further repetition in the sequences of the states of nearest-neighbouring spins in the smaller chains, and the process is repeated until no further subdivision of the smaller chains is possible. This process is comprehensively illustrated in figure 2, where the decomposition of a spin configuration of 30 spins of a spin-1 system is shown. The shaded closed chains, for which no further subdivision is possible, are termed *fundamental spin arrangements*.

The lemma is as follows. The total energy E of an arbitrary spin configuration can be expressed as a linear combination of the energies $\kappa(\theta)\epsilon(\theta)$, corresponding to fundamental

spin arrangements θ, of which the number is finite. $\epsilon(\theta)$ is the energy/spin of the fundamental spin arrangement containing $\kappa(\theta)$ spins. Mathematically,

$$E = \sum_{\theta} \kappa(\theta) n(\theta) \epsilon(\theta) \tag{4}$$

$$N = \sum_{\theta} \kappa(\theta) n(\theta) \tag{5}$$

where N is the total number of spins in the arbitrary spin configuration, and $n(\theta)$ is the number of times the fundamental spin arrangement θ appears in its subdivision.

2.2. The fundamental spin arrangements

As with section 2.1, the discussion is restricted to those fundamental spin arrangements appropriate to systems described by equation (3). The extension to systems with more extended interactions is mentioned in section 4. Because each spin can be in one of $(2S + 1)$ possible states, the total number of different configurations for a pair of spins is $(2S+1)^2$. Since a fundamental spin arrangement cannot (by definition) have a repetition in the sequence of states for a pair of spins, the maximum number of spins in a fundamental spin arrangement is $(2S + 1)^2$.

To find all the possible fundamental spin arrangements we make use of a directed graph of the type used in graph theory [6] . The graphs for the fundamental spin arrangements are constructed by connecting $(2S+1)$ vertices by directed edges. Each vertex represents one of the $(2S + 1)$ spin states and the complete directed graph also has loops connecting a vertex with itself. Each directed edge of this complete directed graph represents the sequence of states for two nearest-neighbouring spins. A fundamental spin arrangement thus corresponds to closed directed looped patterns around the directed edges, without repetition.

The complete directed graph for the $S = \frac{1}{2}$ systems is shown in figure 3. The six looped patterns a, c, $b \to d$, $a \to b \to d$, $b \to c \to d$ and $a \to b \to c \to d$ represent the six fundamental spin arrangements $\uparrow$, $\downarrow$, $\uparrow\downarrow$, $\uparrow\uparrow\downarrow$,$\uparrow\downarrow\downarrow$ and $\uparrow\uparrow\downarrow\downarrow$, with periodic boundary conditions, respectively. This result is in agreement with that of Morita and Horiguchi [5] .

The complete directed graphs for $S = 1$ and $S = \frac{3}{2}$ systems are shown in figures 4(a) and (b), respectively. For a $S = 1$ system, there exist 92 fundamental spin arrangements, listed in figure 5, corresponding to the possible closed clockwise looped patterns of figure 4(a). In figure 5, the fundamental spin arrangements of each length have been divided into three groups. Those of type 'a', are all the ones possessing left–right symmetry in the reversal of the order of the elements (remembering periodic boundary conditions are imposed). The remainder do not exhibit that symmetry. Each of the latter is classed as either type 'b' or type 'c' depending on whether, or not, it, and it's distinct reversed partner, can be used to construct macroscopic degenerate spin configurations (see the next section).

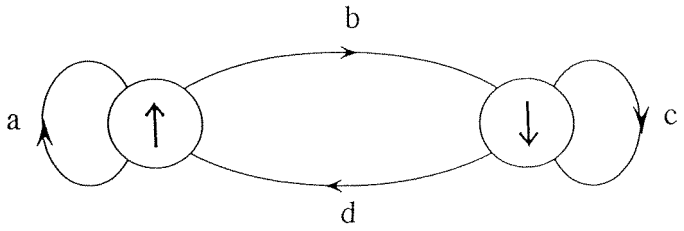

Figure 3. The complete directed graph corresponding to a $S = \frac{1}{2}$ system.

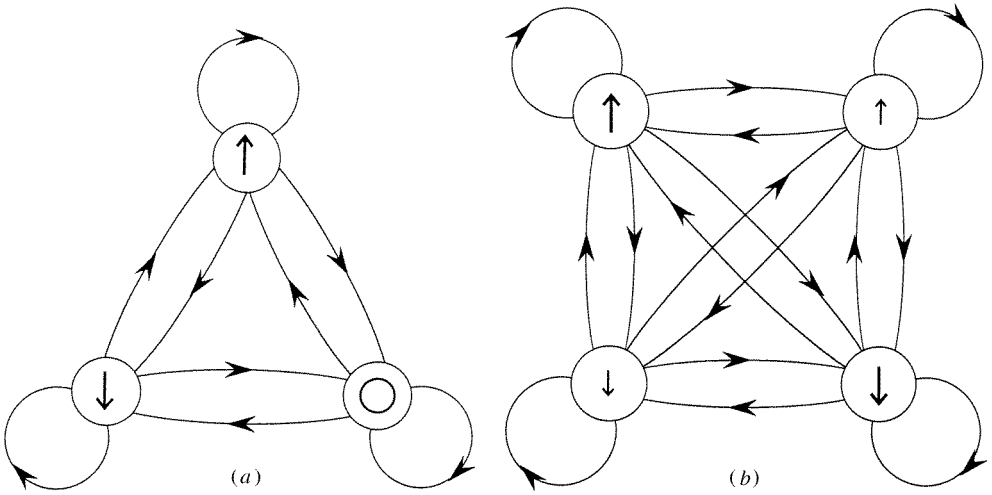

Figure 4. The complete directed graph corresponding to (*a*) a spin-1, (*b*) a spin-$\frac{3}{2}$ system.

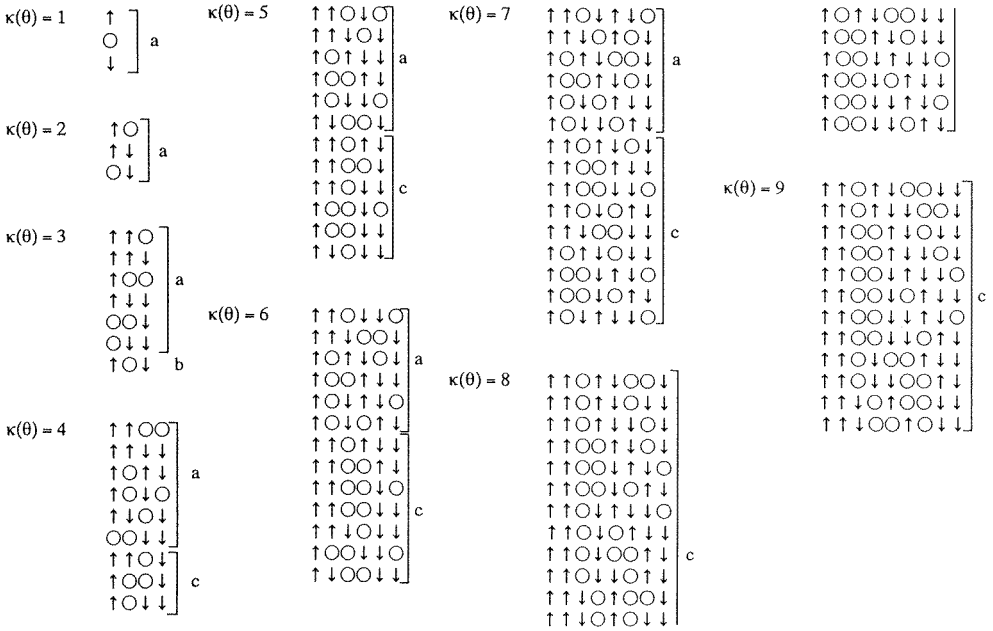

Figure 5. The fundamental spin arrangements for a spin-1 system having nearest- and next-nearest-neighbour interactions.

2.3. The ground state

Just as, in section 2.1, arbitrary spin configurations can be divided into a sum of spin arrangements with the same total energy, fundamental spin arrangements may be used to construct arbitrary spin arrangements whose energy can be the sum of the energies of the fundamental spin arrangements used. Since the ground state of a system is that having the least energy per spin, we can construct it from the fundamental spin arrangements, θ_i^*,

having the least energy per spin of all the fundamental spin arrangements possible, in such a way that the ground-state energy, E, is

$$E = \sum_i \kappa(\theta_i^*) n(\theta_i^*) \epsilon(\theta_i^*) \qquad N = \sum_i \kappa(\theta_i^*) n(\theta_i^*) \,. \tag{6}$$

We consider first the situation when there is a unique θ^*. That is, there is only one fundamental spin arrangement having the lowest energy per spin. Further, if θ^* is of the type 'a', it is seen from the basic dividing rule that equation (6) can be made to hold if we simply join the $n(\theta^*)$ fundamental spin arrangement θ^* end to end, but with the sequence of states in each θ^* occurring in the same order along the chain. As an example, in the spin-1 case, if the fundamental spin arrangement $\uparrow\uparrow\bigcirc\bigcirc$ has the lowest energy per spin, then the ground state is

$$\uparrow\uparrow\bigcirc\bigcirc\ \uparrow\uparrow\bigcirc\bigcirc\uparrow\uparrow\bigcirc\ \bigcirc\cdots.$$

On the other hand, if θ^* had been of type 'b', two possibilities exist since we may use either θ^*, or θ_r^* obtained by left$\leftrightarrow$right reversal in the order of the elements. For example, if θ^* is $\uparrow\bigcirc\downarrow$, then θ_r^* is $\downarrow\bigcirc\uparrow$ and we have the two possibilities

$$\uparrow\bigcirc\downarrow\ \uparrow\bigcirc\downarrow\ \uparrow\bigcirc\downarrow\ \uparrow\bigcirc\downarrow\cdots$$
$$\downarrow\bigcirc\uparrow\ \downarrow\bigcirc\uparrow\ \downarrow\bigcirc\uparrow\ \downarrow\bigcirc\uparrow\cdots.$$

These, of course, are equivalent, the second simply corresponding to the reversal of the chain direction, so it is not a new ground state. We note also, that for this fundamental spin arrangement any spin configuration formed by a combination of θ^* and θ_r^* must lead to a higher energy, as the configuration obtained cannot be subdivided back into just θ^* and θ_r^*'s using the basic dividing rule. The ground state therefore is non-degenerate.

However, if θ^* is one of the fundamental spin arrangements we have labelled 'c', the situation is different. In that case other spin configurations can be constructed from combinations of θ^* and θ_r^* without increasing the energy per spin. For example, with $\theta^* = \uparrow\bigcirc\bigcirc\downarrow$ $(= \bigcirc\bigcirc\downarrow\uparrow)$ and $\theta_r^* = \downarrow\bigcirc\bigcirc\uparrow$ $(= \bigcirc\bigcirc\uparrow\downarrow)$, we may form sequences like

$$\bigcirc\bigcirc\downarrow\uparrow\bigcirc\bigcirc\downarrow\uparrow\bigcirc\bigcirc\uparrow\downarrow\bigcirc\bigcirc\downarrow\uparrow\bigcirc\bigcirc\uparrow\downarrow$$

having the same energy as that configuration

$$\bigcirc\bigcirc\downarrow\uparrow\bigcirc\bigcirc\downarrow\uparrow\bigcirc\bigcirc\downarrow\uparrow\bigcirc\bigcirc\downarrow\uparrow\bigcirc\bigcirc\downarrow\uparrow$$

constructed just from θ^*. This combination of θ^* and θ_r^* leads to a ground state with a macroscopic degeneracy, whose value for this example is given in the next section. We also point out that, since the energy per spin of θ^* and θ_r^* are always the same, independent of the Hamiltonian parameters, this type of degeneracy is generally associated with extended regions of the phase diagram.

The second situation is when there is more than one fundamental spin arrangement θ^* having the same lowest energy per spin. This is the situation that always occurs at a phase boundary, and can again give rise to a macroscopic degeneracy. An example is given in the next section.

3. Magnetic phase diagrams

3.1. One-dimensional models

In this section, exact results for the magnetic phase diagrams of the one-dimensional ANNNI ([2–2]) model described by the Hamiltonian of equation (1), and for the one-dimensional

extended ANNNI ([2–4] and [3–4]) models described by

$$\mathcal{H} = -\sum_i (J_1 S_i S_{i+1} + J_2 S_i^2 S_{i+2}^2 + h S_i) \qquad \text{[2–4] model} \tag{7}$$

$$\mathcal{H} = -\sum_i (J_1 S_i S_{i+1} + J_2 S_i S_{i+1}^2 S_{i+2} + h S_i) \qquad \text{[3–4] model} \tag{8}$$

are obtained using the methods described above. In the [2–4] and [3–4] models the higher-order spin interactions, $S_i^2 S_{i+2}^2$ (the biquadratic interaction) and $S_i S_{i+1}^2 S_{i+2}$ (the three-site four-spin interaction), are considered as next-nearest-neighbour interactions [7] .

The magnetic ground-state phase diagrams for the $S = \frac{1}{2}$ [2–2] model are shown in figure 6. Although plotted in a different parameter space, it can be shown that they are consistent with the phase diagram of Morita and Horiguchi [5] . The same magnetic phase diagram (apart from scaling) is also obtained for the $S = 1$ [2–2] model. In fact, the ground state of the one-dimensional [2–2] model with arbitrary spin quantum number S may be described by the following reduced Hamiltonian:

$$\mathcal{H}_{\text{red}} = -S^2 \sum_i \left(J_1 \sigma_i \sigma_{i+1} + J_2 \sigma_i \sigma_{i+2} + \frac{h}{S} \sigma_i \right), \tag{9}$$

where $\sigma_i = \pm 1$. Thus by using the reduced field $h/S|J_1|$, figure 6 gives the ground-state phase diagram for arbitrary spin quantum number S. The coordinates $(J_2/|J_1|, h/S|J_1|)$ of the multiphase points are

$$\text{A}: \left(-\tfrac{1}{2}, 0\right) \qquad \text{A}^{\pm}: \ (0, \pm 2) \qquad \text{B}^{\pm}: \left(-\tfrac{1}{2}, 0\right). \tag{10}$$

Also, the phase boundaries are as follows:
For $J_1 > 0$,

$$(\uparrow) - (\downarrow) : h = 0 \qquad (\uparrow) - (\uparrow\uparrow\downarrow\downarrow) : J_1 + 2J_2 + (h/S) = 0\,. \tag{11}$$

For $J_1 < 0$,

$$\begin{aligned} &(\uparrow) - (\uparrow\downarrow) : 2|J_1| - (h/S) = 0 \qquad (\uparrow) - (\uparrow\uparrow\downarrow) : 2|J_1| - 2J_2 - (h/S) = 0 \\ &(\uparrow\uparrow\downarrow) - (\uparrow\uparrow\downarrow\downarrow) : |J_1| + 2J_2 + (h/S) = 0\,. \end{aligned} \tag{12}$$

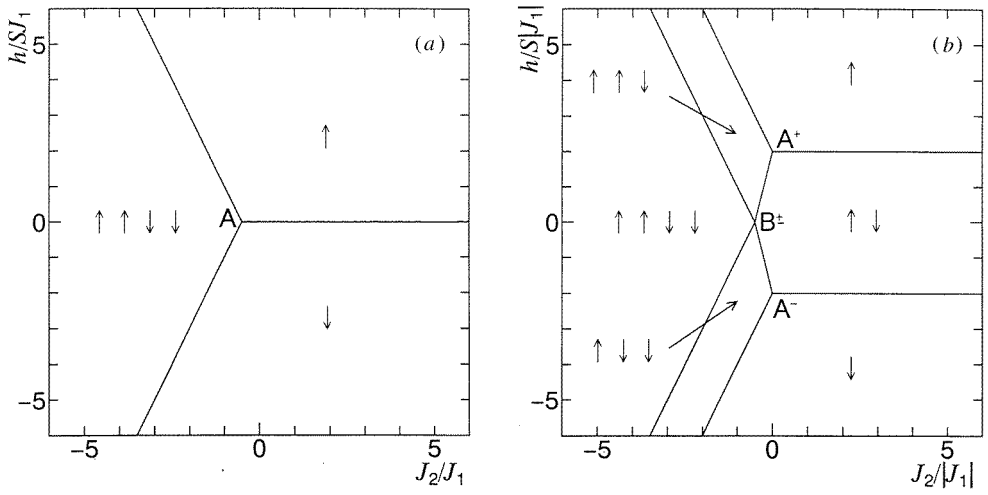

Figure 6. The ground-state phase diagram of the ANNNI [2–2] model with arbitrary spin. (*a*) and (*b*) are for $J_1 > 0$ and $J_1 < 0$, respectively.

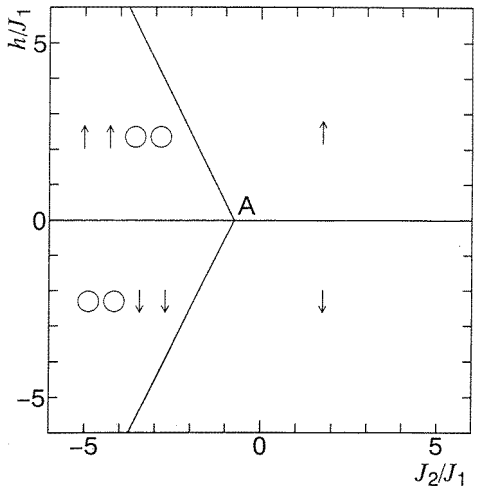

Figure 7. The ground-state phase diagram for the $S = 1$ [2–4] model with $J_1 > 0$, in the case when $zJ_0 = 0$.

The other phase boundaries can be obtained by symmetry, or from the coordinates of the multiphase points given in equation (10).

The ground-state phase diagrams for the $S = 1$ [2–4] and [3–4] models are shown in figures 7 and 8, and in figure 9, respectively. The salient features of these phase diagrams are described in the next section dealing with two- and three-dimensional models in which interchain coupling is also included. The result for the $S = 1$ [3–4] model with $J_1 > 0$, in the special case when $h = 0$, is in agreement with that obtained by the transfer matrix method [3]. As a check on our technique, we have compared the phase diagrams with those deduced from the results of a computer search of the ground-state configurations of finite chains up to twelve spins long. The results agree.

The ground-state degeneracy at the phase boundaries in the ANNNI model has been discussed in [8]. Similar considerations apply to the phase boundaries in the [2–4] and [3–4] models. As an example, we consider the phase boundary between the $\uparrow$ phase and the $\uparrow\uparrow \bigcirc\bigcirc$ phase in figure 7. On the boundary, any sequence of the fundamental spin arrangements $\uparrow$ and $\uparrow\uparrow \bigcirc\bigcirc$ along the chain has the same ground-state energy, since the $\epsilon_{\uparrow}$ and $\epsilon_{\uparrow\uparrow\bigcirc\bigcirc}$ are degenerate at the phase boundary. Letting D_N denote the ground-state degeneracy of an N-spin system, the recurrence relation

$$D_N = D_{N-1} + D_{N-4} \tag{13}$$

is obtained. In the thermodynamic limit, we find the remanent entropy is given by

$$\lim_{N\to\infty} \frac{1}{N} \ln(D_N) = \ln(\chi) \approx 0.322\,28 \tag{14}$$

where χ is the solution of the quartic equation $\chi^3(\chi - 1) = 1$. Due to symmetry, the same result also applies to the boundary between the $\downarrow$ and $\bigcirc\bigcirc\downarrow\downarrow$ phases.

Macroscopic ground-state degeneracies can exist within a region of the phase diagram, as was pointed out in [4] in the case of the triangular antiferromagnet. For example, the phase labelled $\uparrow \bigcirc\bigcirc \downarrow$ in figure 8(a) has a degeneracy for the reasons discussed in section 2.3. In this case, the recurrence relation

$$D_N = 2D_{N-4} \tag{15}$$

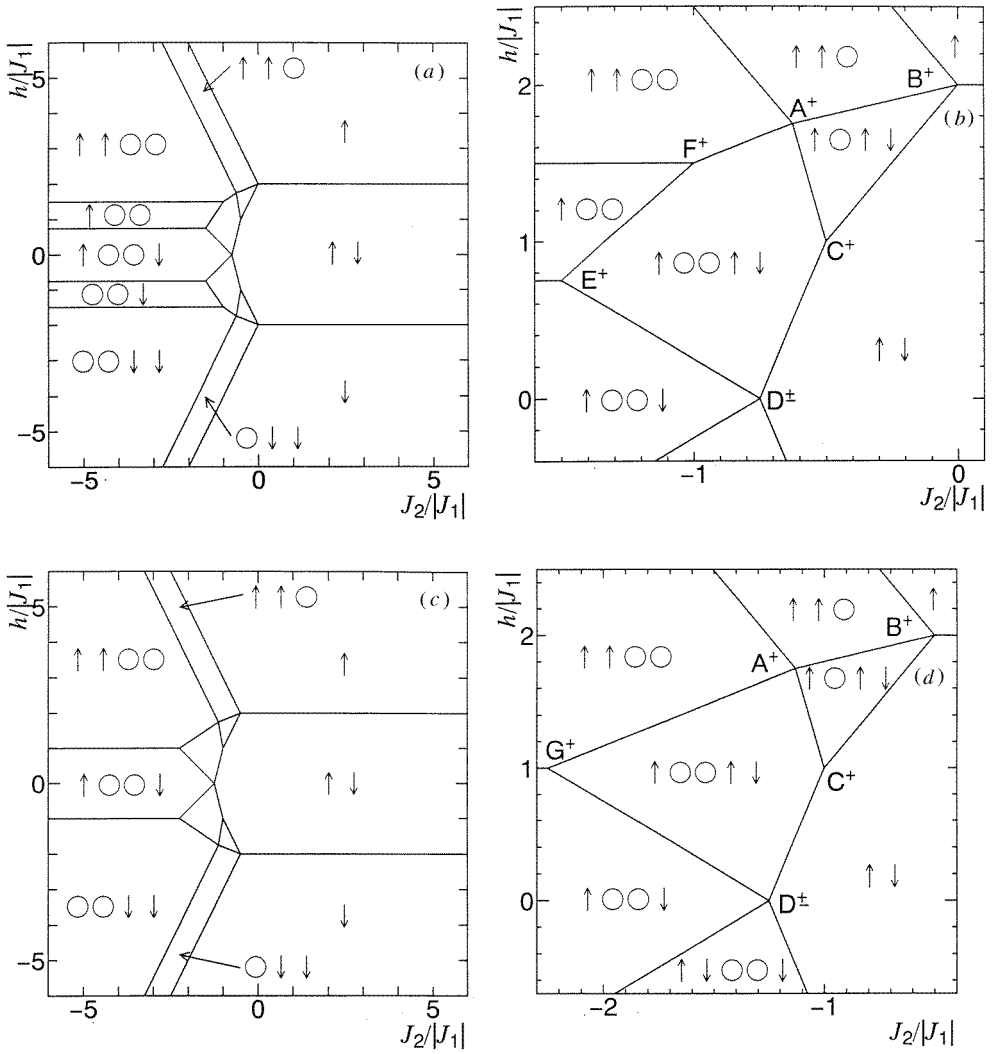

Figure 8. The ground-state phase diagram for the $S = 1$ [2–4] model with $J_1 < 0$. (*a*) and (*c*) correspond to $zJ_0/|J_1| = 0$ and 2, respectively. Portions of these diagrams are expanded in (*b*) and (*d*), respectively, to show the labelling of the multiphase points.

holds, and the remanent entropy is

$$\lim_{N\to\infty} \frac{1}{N} \ln(D_N) = \frac{1}{4} \ln(2) \,. \tag{16}$$

3.2. Axial two- and three-dimensional models with ferromagnetic interchain coupling

In this section we report results for the magnetic ground-state phase diagrams of axial two- and three-dimensional models having ferromagnetic interchain coupling [3, 9, 10], described

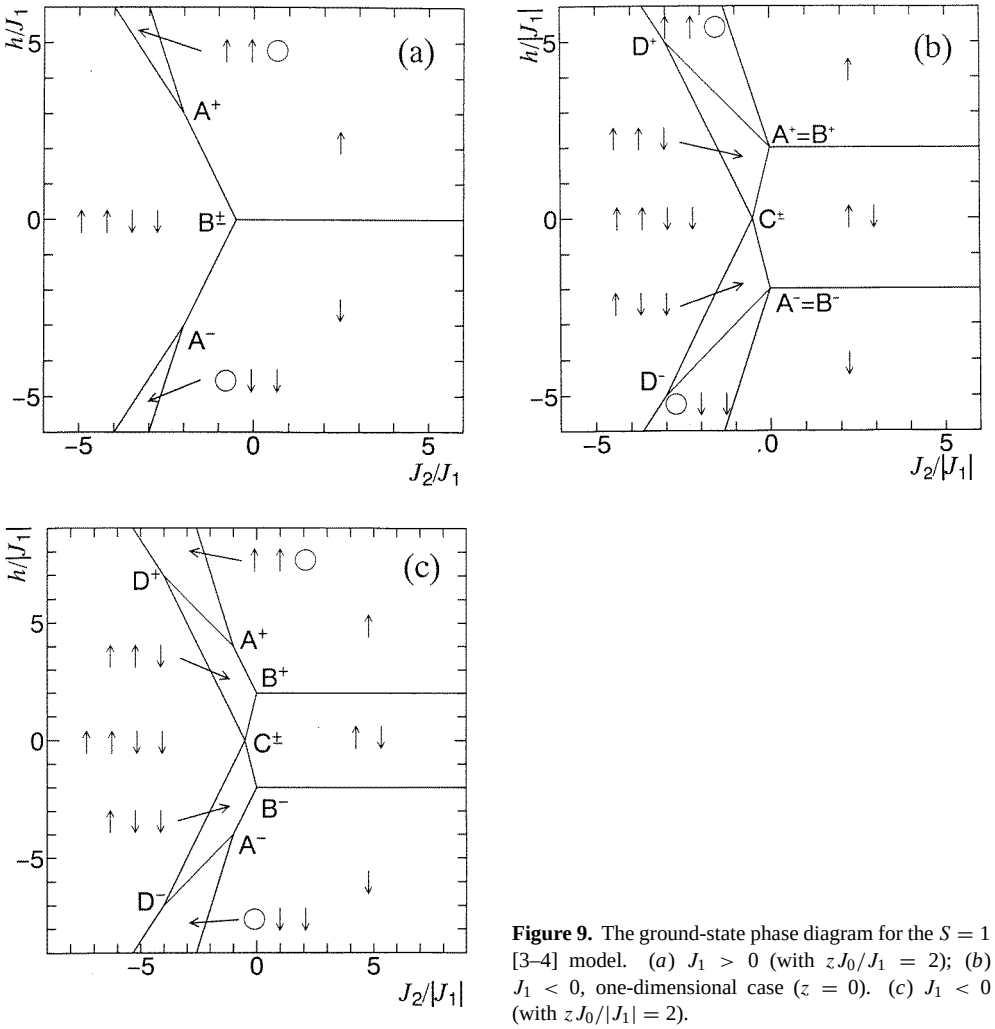

Figure 9. The ground-state phase diagram for the $S = 1$ [3–4] model. (*a*) $J_1 > 0$ (with $zJ_0/J_1 = 2$); (*b*) $J_1 < 0$, one-dimensional case ($z = 0$). (*c*) $J_1 < 0$ (with $zJ_0/|J_1| = 2$).

by the Hamiltonians

$$\mathcal{H} = -\sum_i \sum_j \left[\frac{J_0}{2} \left(\sum_{k=1}^{z} S_{i,j} S_{i,k} \right) + J_1 S_{i,j} S_{i+1,j} + J_2 S_{i,j} S_{i+2,j} + h S_{i,j} \right]$$

[2–2] model (17)

$$\mathcal{H} = -\sum_i \sum_j \left[\frac{J_0}{2} \left(\sum_{k=1}^{z} S_{i,j} S_{i,k} \right) + J_1 S_{i,j} S_{i+1,j} + J_2 S_{i,j}^2 S_{i+2,j}^2 + h S_{i,j} \right]$$

[2–4] model (18)

$$\mathcal{H} = -\sum_i \sum_j \left[\frac{J_0}{2} \left(\sum_{k=1}^{z} S_{i,j} S_{i,k} \right) + J_1 S_{i,j} S_{i+1,j} + J_2 S_{i,j} S_{i+1,j}^2 S_{i+2,j} + h S_{i,j} \right]$$

[3–4] model. (19)

These models are composed of chains of spins parallel to the *c*-axis (say), and nearest-neighbouring chains interact through an interchain exchange interaction. The discussion will

be confined to those lattices for which each spin in a chain has only one nearest-neighbouring spin in each of the nearest-neighbouring chains, and they lie in a plane perpendicular to the c-axis through the spin in question. J_0 is the interchain exchange coupling between those spins. The summations over i and j are over all the spins along the chain, and in the c-plane, respectively. The summation over k is over the z nearest neighbours of j in the c-plane. For example, z is 2 and 4 for square and simple cubic lattices, respectively. (It is understood that the first term in equations (17)–(19) is to be omitted when $z = 0$, corresponding to uncoupled one-dimensional chains).

For ferromagnetic interchain coupling ($J_0 > 0$), it is believed that all the spins within the c-plane are stabilized in the same spin state, that is, there exists no phase shift along the c-axis between the spin configurations of the different chains. Therefore, the ground state in each model can be described by the following chain Hamiltonians,

$$\mathcal{H}_c = -\sum_i \left(\frac{zJ_0}{2} S_i^2 + J_1 S_i S_{i+1} + J_2 S_i S_{i+2} + hS_i \right) \qquad \text{[2–2] model} \tag{20}$$

$$\mathcal{H}_c = -\sum_i \left(\frac{zJ_0}{2} S_i^2 + J_1 S_i S_{i+1} + J_2 S_i^2 S_{i+2}^2 + hS_i \right) \qquad \text{[2–4] model} \tag{21}$$

$$\mathcal{H}_c = -\sum_i \left(\frac{zJ_0}{2} S_i^2 + J_1 S_i S_{i+1} + J_2 S_i S_{i+1}^2 S_{i+2} + hS_i \right) \qquad \text{[3–4] model}. \tag{22}$$

Thus when $J_0 > 0$, these models are essentially one-dimensional models and their magnetic phase diagrams can be rigorously determined using the theory of the previous sections.

As for the one-dimensional case, the ground state of the two- and three-dimensional [2–2] model with arbitrary spin quantum number S may be described by a reduced Hamiltonian,

$$\mathcal{H}_{\text{red}} = -\frac{zNJ_0S^2}{2} - S^2 \sum_i \left(J_1 \sigma_i \sigma_{i+1} + J_2 \sigma_i \sigma_{i+2} + \frac{h}{S} \sigma_i \right) \tag{23}$$

where $\sigma_i = \pm 1$, and N is the chain length. The interchain coupling, J_0, thus only appears in a constant term in the reduced Hamiltonian and so does not change the picture of the ground-state phase diagram. Figure 6 thus holds for the two- and three-dimensional models being considered, as well as for the one-dimensional case.

The magnetic phase diagram for the $S = 1$ [2–4] model when the axial bilinear exchange interaction J_1 is ferromagnetic is shown in figure 7 (drawn for the case when $zJ_0 = 0$). The coordinates $(J_2/J_1, h/J_1)$ of the multiphase point A, and the equations of the phase boundaries are given by

$$\text{A}: \left(-\frac{3}{4} - \frac{zJ_0}{4J_1}, 0 \right) \tag{24}$$

$$(\uparrow) - (\downarrow): \; h = 0 \qquad (\uparrow) - (\uparrow\uparrow \bigcirc\bigcirc): \; 3J_1 + 4J_2 + 2h + zJ_0 = 0\,. \tag{25}$$

It is seen that increasing zJ_0 only translates the picture to the left, so the phase diagram is topologically invariant with respect to the dimensionality and to the interchain coupling.

For the antiferromagnetic case, $J_1 < 0$, the situation is much more complicated, as shown in figure 8. When the effective interchain coupling is relatively small, $0 \leqslant zJ_0/|J_1| < 1$, the phase diagram is as shown in figure 8(a). (This figure is drawn for the case of $zJ_0 = 0$.) An expanded portion of the inner part of the phase diagram is shown in figure 8(b), for clarity of labelling. The coordinates $(J_2/|J_1|, h/|J_1|)$ of the multiphase

points are as follows:

$$\begin{aligned}
&\mathrm{A}^{\pm}:\ \left(-\frac{5}{8}-\frac{zJ_0}{4|J_1|},\pm\frac{7}{4}\right) \qquad \mathrm{B}^{\pm}:\ \left(-\frac{zJ_0}{4|J_1|},\pm 2\right)\\
&\mathrm{C}^{\pm}:\ \left(-\frac{1}{2}-\frac{zJ_0}{4|J_1|},\pm 1\right) \qquad \mathrm{D}^{\pm}:\ \left(-\frac{3}{4}-\frac{zJ_0}{4|J_1|},0\right)\\
&\mathrm{E}^{\pm}:\ \left(-\frac{3}{2}-\frac{zJ_0}{2|J_1|},\pm\frac{3}{4}\pm\frac{zJ_0}{4|J_1|}\right)\\
&\mathrm{F}^{\pm}:\ \left(-1-\frac{zJ_0}{|J_1|},\pm\frac{3}{2}\mp\frac{zJ_0}{2|J_1|}\right).
\end{aligned} \tag{26}$$

With increase in zJ_0, all the points $\mathrm{A}^{\pm}$, $\mathrm{B}^{\pm}$, $\mathrm{C}^{\pm}$, $\mathrm{D}^{\pm}$ translate horizontally to the left in this picture by the same amount, $zJ_0/4|J_1|$. However, as the effective interchain coupling, zJ_0, increases, the multiphase points E^{+} and F^{+} approach each other (as also do E^{-} and F^{-}). The phases $\uparrow\bigcirc\bigcirc$ and $\bigcirc\bigcirc\downarrow$ become increasingly narrow and eventually disappear when the points $\mathrm{E}^{\pm}$ and $\mathrm{F}^{\pm}$ coalesce at $J_2/|J_1| = -2$, $h = \pm 1$. This occurs at the critical value $zJ_0/|J_1| = 1$. Above this critical value of the effective interchain coupling strength, the phase diagram is as shown in figures 8(*c*) and (*d*) (plotted for the case $zJ_0/|J_1| = 2$). The coordinates $(J_2/|J_1|, h/|J_1|)$ of the multiphase points $\mathrm{G}^{\pm}$ (figure 8(*d*)) that arose from the merger of $\mathrm{E}^{\pm}$ and $\mathrm{F}^{\pm}$ of figure 8(*b*) are

$$\mathrm{G}^{\pm}:\ \left(-\frac{7}{4}-\frac{zJ_0}{4|J_1|},\pm 1\right). \tag{27}$$

The phase boundaries in figure 8, that cannot be deduced from the coordinates of the multiphase points given above, are

$$\begin{aligned}
&(\uparrow)-(\uparrow\uparrow\bigcirc):\ 2|J_1|-2J_2-h-(zJ_0/2)=0\\
&(\uparrow\uparrow\bigcirc)-(\uparrow\uparrow\bigcirc\bigcirc):\ |J_1|-4J_2-2h-zJ_0=0
\end{aligned} \tag{28}$$

with those for negative h deduced by symmetry.

The magnetic phase diagrams for the spin-1 [3–4] models are shown in figure 9. With a ferromagnetic axial bilinear exchange interaction J_1 the situation is as in figure 9(*a*) (drawn for the case when $zJ_0/J_1 = 2$). The coordinates $(J_2/J_1, h/J_1)$ of the multiphase points, and the phase boundaries are

$$\mathrm{A}^{\pm}:\ \left(-1-\frac{zJ_0}{2J_1},\pm 1\pm\frac{zJ_0}{J_1}\right) \qquad \mathrm{B}^{\pm}:\ \left(-\frac{1}{2},0\right) \tag{29}$$

$$\begin{aligned}
&(\uparrow)-(\uparrow\uparrow\bigcirc):\ 2J_1+3J_2+h+(zJ_0/2)=0\\
&(\uparrow\uparrow\bigcirc)-(\uparrow\uparrow\downarrow\downarrow):\ J_1+3J_2+2h-(zJ_0/2)=0\,.
\end{aligned} \tag{30}$$

The point $\mathrm{B}^{\pm}$ is independent of the dimensionality and strength of the interchain coupling, whilst the points $\mathrm{A}^{\pm}$ move to lower values of J_2 and occur at higher values of $|h|$ as zJ_0 increases.

On the other hand, when the axial bilinear exchange interaction J_1 is antiferromagnetic ($J_1 < 0$) the situation is different for the one-dimensional and for the two- and three-dimensional cases. The former is shown in figure 9(*b*), where the coordinates $(J_2/|J_1|, h/|J_1|$ of the multiphase points are

$$\mathrm{A}^{\pm}=\mathrm{B}^{\pm}:(0,\pm 2) \qquad \mathrm{C}^{\pm}:(-\tfrac{1}{2},0) \qquad \mathrm{D}^{\pm}:(-3,\pm 5)\,. \tag{31}$$

For the two- and three-dimensional cases, the $\mathrm{B}^{\pm}$ split away from $\mathrm{A}^{\pm}$ as shown in figure 9(*c*) (drawn for $zJ_0/|J_1| = 2$) and new phase boundaries between the $\uparrow\uparrow\downarrow$ and $\uparrow$ phases, and

between the $\uparrow\downarrow\downarrow$ and $\downarrow$ phases, appear. The coordinates $(J_2/|J_1|, h/|J_1|)$ of the multiphase points are as follows:

$$\begin{aligned} &\mathrm{A}^{\pm}: \left(-\frac{zJ_0}{2|J_1|}, \pm 2 \pm \frac{zJ_0}{|J_1|}\right) \qquad \mathrm{B}^{\pm}: (0, \pm 2) \qquad \mathrm{C}^{\pm}: (-\tfrac{1}{2}, 0) \\ &\mathrm{D}^{\pm}: \left(-3 - \frac{zJ_0}{|J_1|}, \pm 5 \pm \frac{zJ_0}{|J_1|}\right). \end{aligned} \tag{32}$$

Thus the coordinates of $\mathrm{B}^{\pm}$ and $\mathrm{C}^{\pm}$ are independent of the interchain coupling and the relative separation of $\mathrm{A}^{\pm}$ and $\mathrm{D}^{\pm}$ remains fixed. The phase boundaries in figures 9(*b*) and (*c*), that cannot be inferred from the coordinates of the multiphase points given above, are

$$\begin{aligned} &(\uparrow) - (\uparrow\uparrow\bigcirc): |4|J_1| - 6J_2 - 2h - J_0 = 0 \\ &(\uparrow\uparrow\bigcirc) - (\uparrow\uparrow\downarrow\downarrow): 2|J_1| - 6J_2 - 4h + zJ_0 = 0\,. \end{aligned} \tag{33}$$

4. Conclusions

In this paper, by adopting the concept of fundamental spin arrangements we have proposed a lemma applicable to the calculation of the ground state of all one-dimensional ANNNI models of arbitrary spin with various nearest- and next-nearest-neighbour interactions. As well as deriving the lemma, a prescription for the construction of all the fundamental spin arrangements has been given, and they have been listed for $S = \frac{1}{2}$ and $S = 1$. The lemma has been applied to determine the exact ground state for the ANNNI [2–2] model of arbitrary spin, and the $S = 1$ ANNNI [2–4] and [3–4] models in one, two and three dimensions. We have checked our results by numerical simulation of the ground states of finite chains.

Yamada and Hamaya [11] have shown that the phase structure of a large number of ferroelectric materials can be explained using an ANNNI model extended to include axial third-nearest-neighbour interactions (i.e. the A3NNI model). It thus seems that the ground states for systems with more distant nearest-neighbour interactions than those we have considered above, are also important in some physical situations [12–14] .

The necessary modifications to the above theory for these systems are as follows. First, for systems having third- and fourth-nearest-neighbour interactions our basic dividing rule, presented in section 2.1, has to be modified. Instead of basing it on the repetition in states of pairs of nearest-neighbouring spins, it has to based on the repetition in states of triplets and quartets of spins, respectively. In general, for a system with nth-nearest-neighbour interactions one has to look for repetitions in states along the chain in clusters of n spins. Secondly, for nth-nearest-neighbour interactions the maximum number of spins in a fundamental spin arrangement has to be increased from $(2S+1)^2$, as was the case in section 2.2, to $(2S+1)^n$, which is the total number of different configurations for a cluster of n spins. The set of fundamental spin arrangements is obtained by the combination of these $(2S+1)^n$ arrangements, without repetition. For an $S = \frac{1}{2}$ system with third- and fourth-nearest-neighbour interactions there exist 15 and 106 fundamental spin arrangements, respectively. Using these fundamental spin arrangements it is possible to determine the magnetic phase diagrams for Ising models with couplings to such distant axial nearest neighbours.

The ground states of $S \geqslant \frac{3}{2}$ extended ANNNI models can be obtained in the same way. For the case of $S = \frac{3}{2}$, for example, there appear 60 487 fundamental spin arrangements up to 16 spins in length, and we have found that in both the [2–4] and [3–4] models, increasing the magnitude of S causes considerable changes, and complications to the magnetic phase

diagram. These changes may be attributed to the non-linearity of the higher-order spin interactions.

Although in this paper attention has been focused on the ground state, it is an attractive problem to study the behaviour of the extended ANNNI models at finite temperature. Monte Carlo simulation [3] and molecular field calculations [9] have shown that the $S = 1$ three-dimensional [2–2] model is qualitatively similar to that of the $S = \frac{1}{2}$ ANNNI model [1]. In the three-dimensional [3–4] model, a molecular field calculation [10] has shown that a re-entrant phase transition exists near the multicritical point and the devil's flower is partially destroyed around the multicritical point for $S > 1$. For this model with $S > 1$, a Monte Carlo simulation is now in progress which should clarify the situation regarding the existence of the re-entrant phase transition. Also, for the three-dimensional [2–4] model, a molecular field calculation and a Monte Carlo simulation are in progress. From these calculations the role of higher order spin interactions in frustrated systems should become clearer.

Acknowledgments

The numerical calculations were partially carried out at the Computer Centre, Kyushu University. The authors would like to express their sincere thanks to Professor K Takeda for his valuable discussions.

References

[1] Selke W 1988 *Phys. Rep.* **170** 213–64
[2] Thompson J 1972 *Phase Transitions and Critical Phenornena* vol I, ed C Domb and M S Green (New York: Academic) pp 177–26
[3] Muraoka Y, Ochiai M, Idogaki T and Uryu N 1993 *J. Phys. A: Math. Gen.* **26** 1811–21
[4] Wannier G H 1950 *Phys. Rev.* **79** 357–64
[5] Morita T and Horiguchi T 1972 *Phys. Lett.* **38A** 223–4
[6] Bondy J A and Murty U S R 1976 *Graph Theory with Applications* (London: Macmillan)
[7] Iwashita T and Uryu N 1979 *J. Phys. Soc. Japan* **47** 786–9. See also other references cited therein.
[8] Yokoi C S O, Coutinho-Filho M D and Salinas S R 1981 *Phys. Rev.* B **24** 4047–61
[9] Muraoka Y, Ochiai M and Idogaki T 1994 *J. Phys. A: Math. Gen.* **27** 2675–86
[10] Muraoka Y, Ochiai M and Idogaki T 1995 *J. Magn. Magn. Mater.* **140–144** 1489–90
[11] Yamada Y and Hamaya N 1983 *J. Phys. Soc. Japan* **52** 3466–74
[12] Selke W, Barreto M and Yeomans J 1985 *J. Phys. C: Solid State Phys.* **18** L393–9
[13] Randa J 1985 *Phys. Rev.* B **32** 413–6
[14] Hassold G N, Dreitlein J F, Beale P D and Scott J F 1986 *Phys. Rev.* B **33** 3581–4